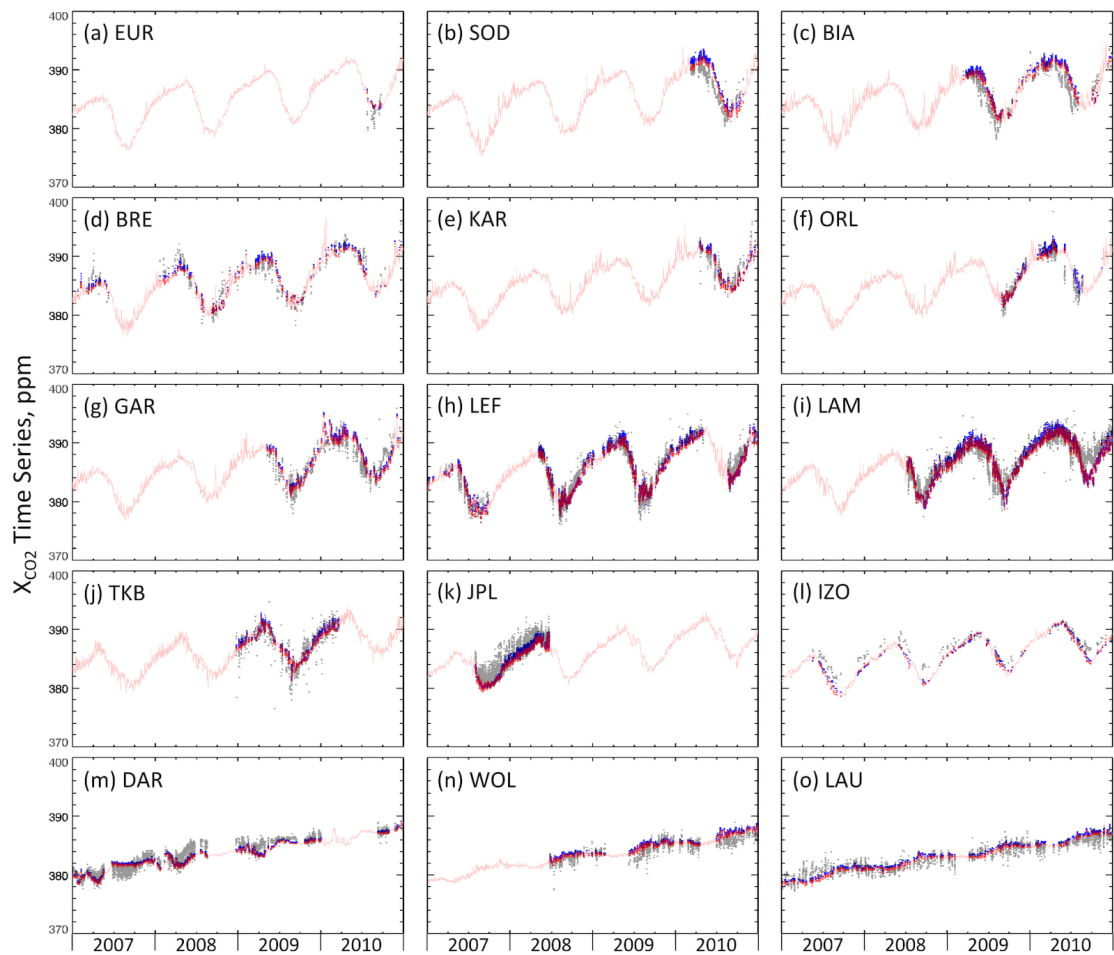


## Supplementary materials for

# "Technical Note: Latitude-time variations of atmospheric column-average dry air mole fractions of CO<sub>2</sub>, CH<sub>4</sub> and N<sub>2</sub>O"

Ryu Saito<sup>1</sup>, Prabir K. Patra<sup>1</sup>, Nicholas Deutscher<sup>2,6</sup>, Debra Wunch<sup>3</sup>, Kentaro Ishijima<sup>1</sup>, Vanessa Sherlock<sup>4</sup>, Thomas Blumenstock<sup>5</sup>, Susanne Dohe<sup>5</sup>, David Griffith<sup>6</sup>, Frank Hase<sup>5</sup>, Pauli Heikkinen<sup>7</sup>, Esko Kyrö<sup>7</sup>, Ronald Macatangay<sup>6</sup>, Joseph Mendonca<sup>8</sup>, Janina Messerschmidt<sup>3</sup>, Isamu Morino<sup>9</sup>, Justus Notholt<sup>2</sup>, Markus Rettinger<sup>10</sup>, Kimberly Strong<sup>8</sup>, Ralf Sussmann<sup>10</sup>, and Thorsten Warneke<sup>2</sup>



**Figure S1:** Comparisons of TCCON measurement (black dots) and ACTM-simulation smoothed by averaging kernels and a priori profiles (red dots) for X<sub>CO<sub>2</sub></sub> at all the sites considered in this study. Only a sub-set of sites are presented in Fig. 4.

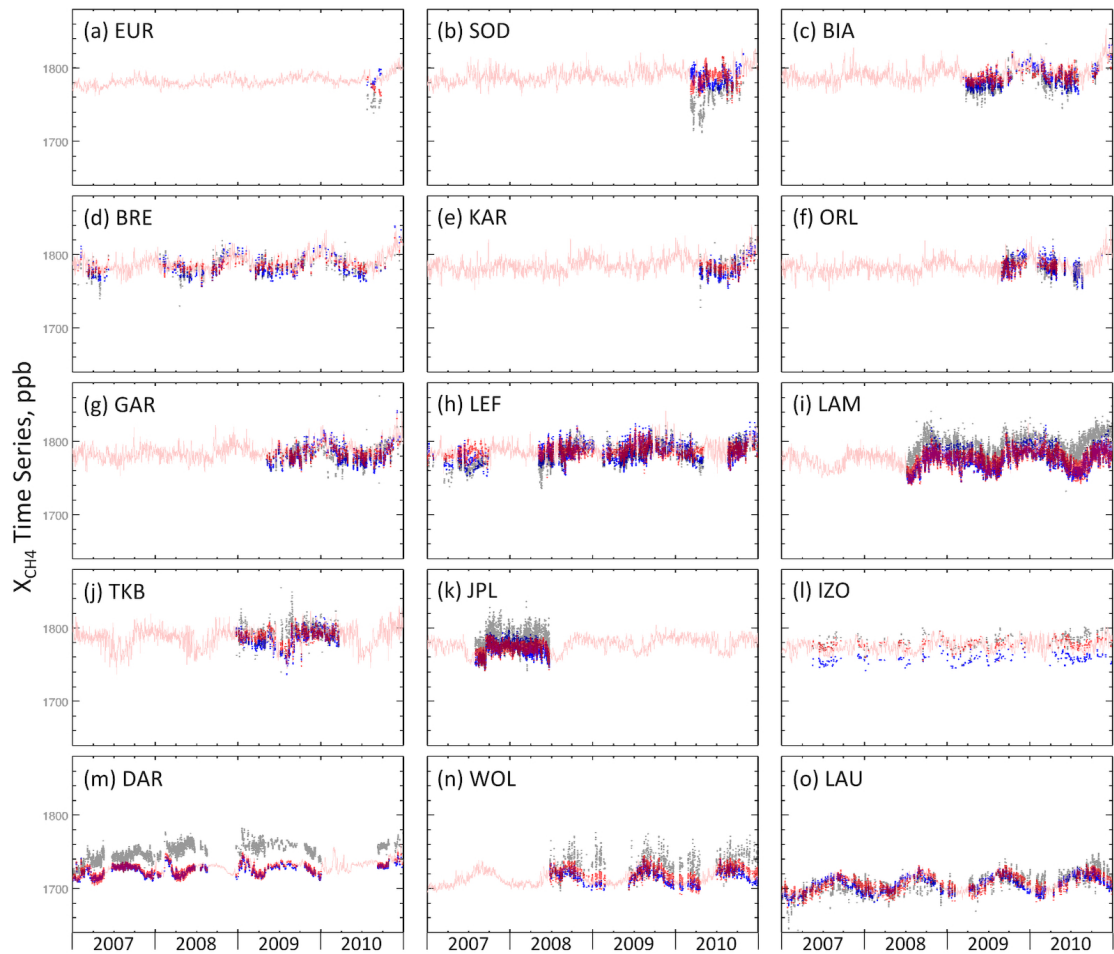


**Figure S2:** Same as Fig. S1, but for time series of X<sub>CH4</sub>.

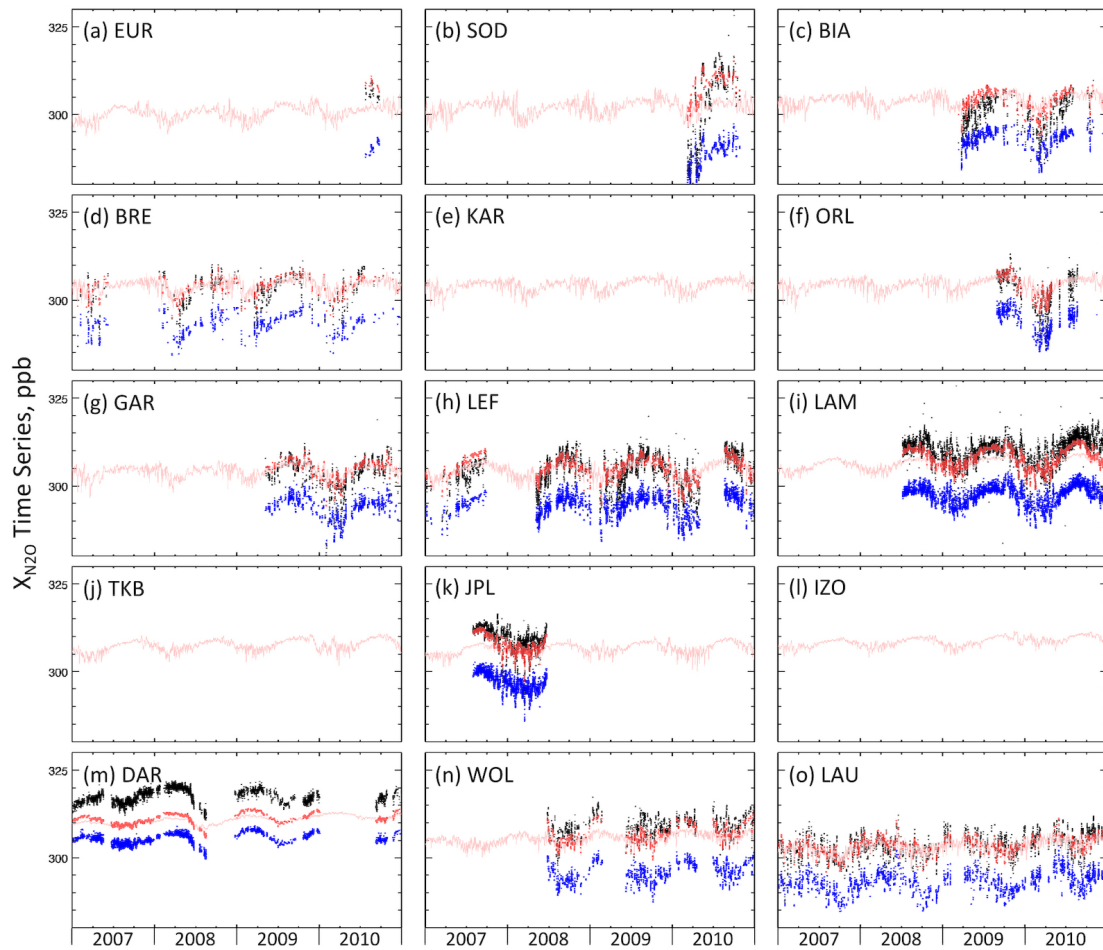


**Figure S3:** Same as Fig. S1, but for time series of  $X_{N2O}$ .

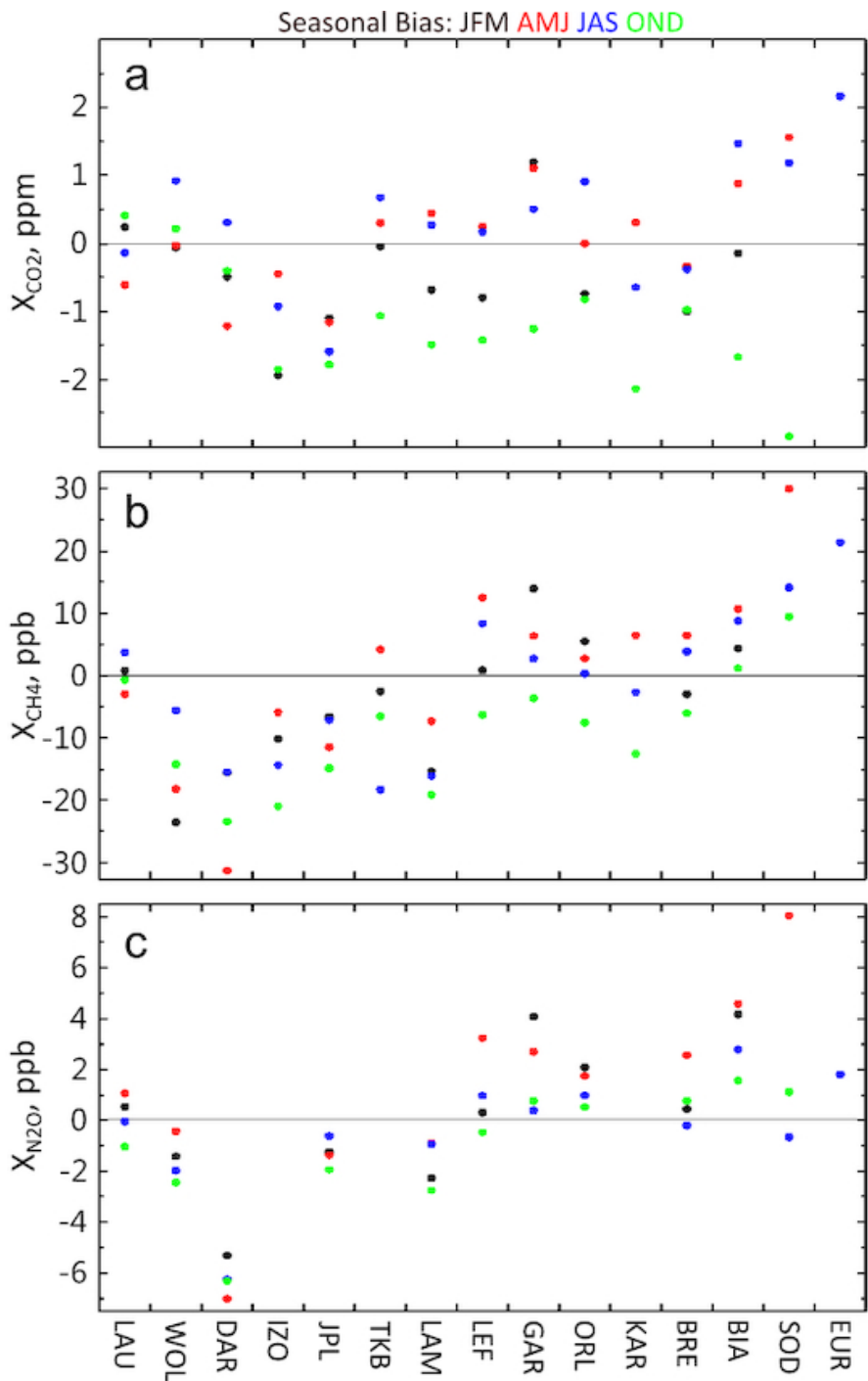


**Figure S4:** Variations in bias  $b$  between seasons: January-March (JFM; black), April-June (AMJ; red), July-September (JAS; blue) and October-December (OND; green).

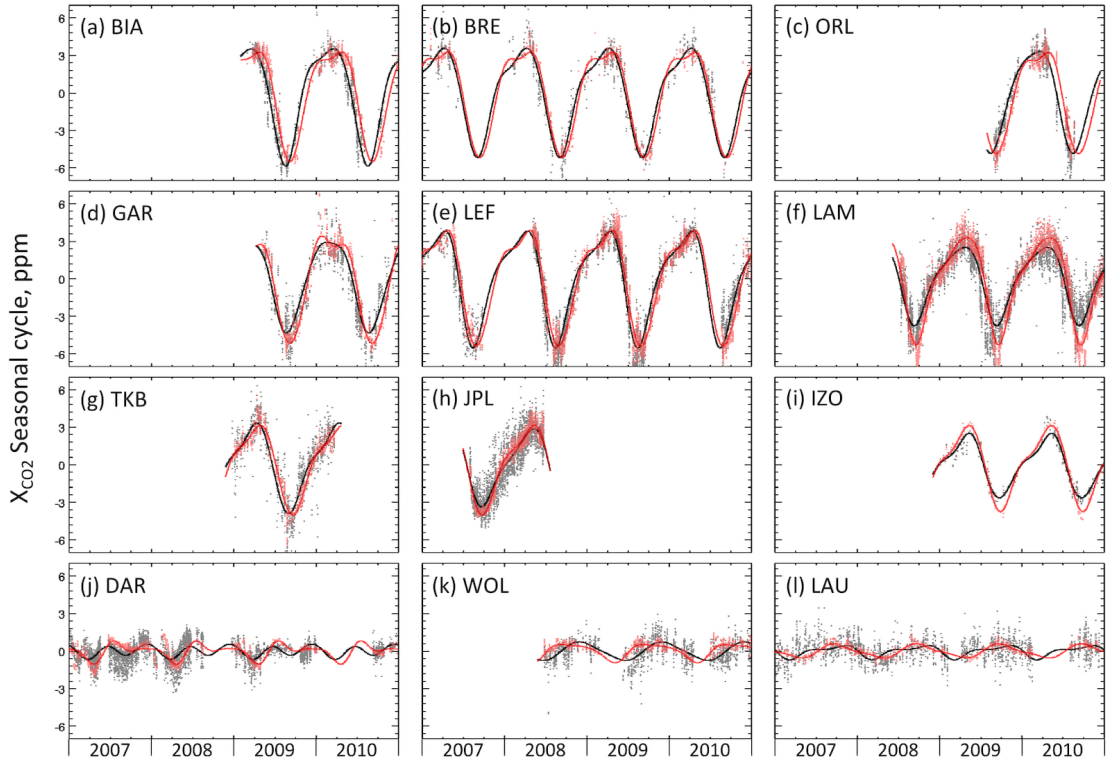


**Figure S5:** Seasonal cycles of  $X_{CO_2}$  are compared for ACTM and TCCON time series (smoothed lines for [fitted curve – long-term trends], and dots are for [original time series – long-term trends]). The seasonal cycles for EUR, SOD and KAR are not depicted because the time series are too short for fitting (ref. main text).

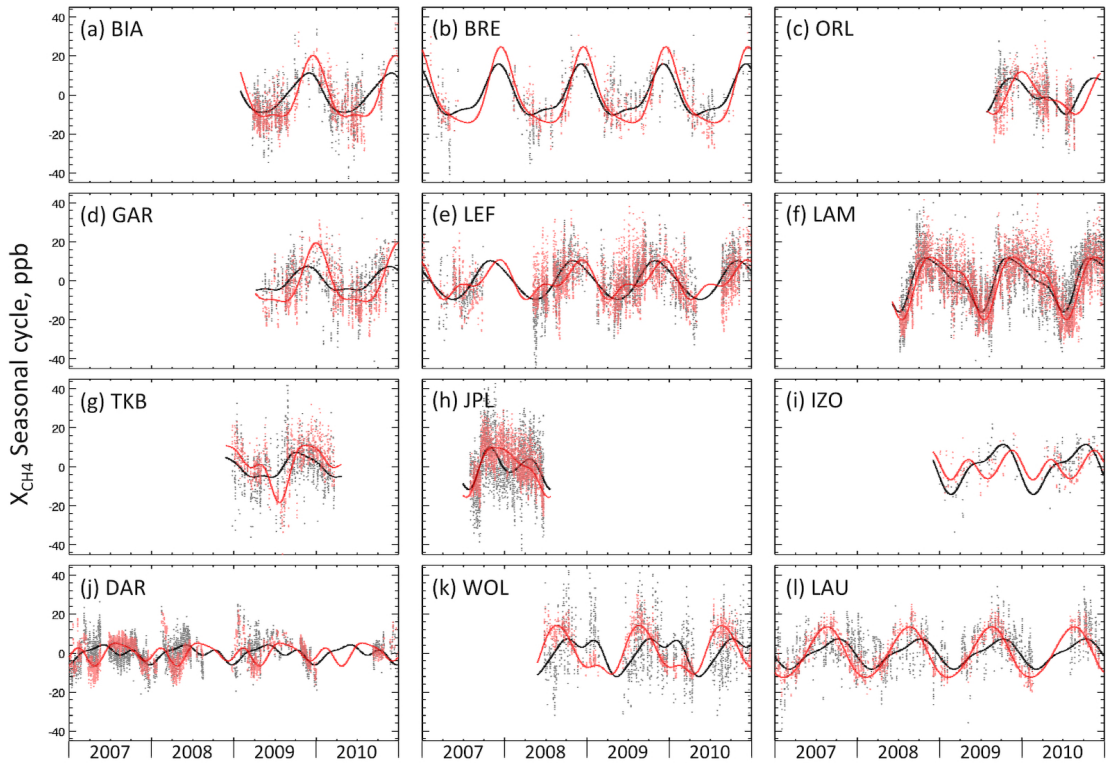


**Figure S6:** Same as Fig. S5, but the seasonal cycles of  $X_{\text{CH}_4}$  are shown.

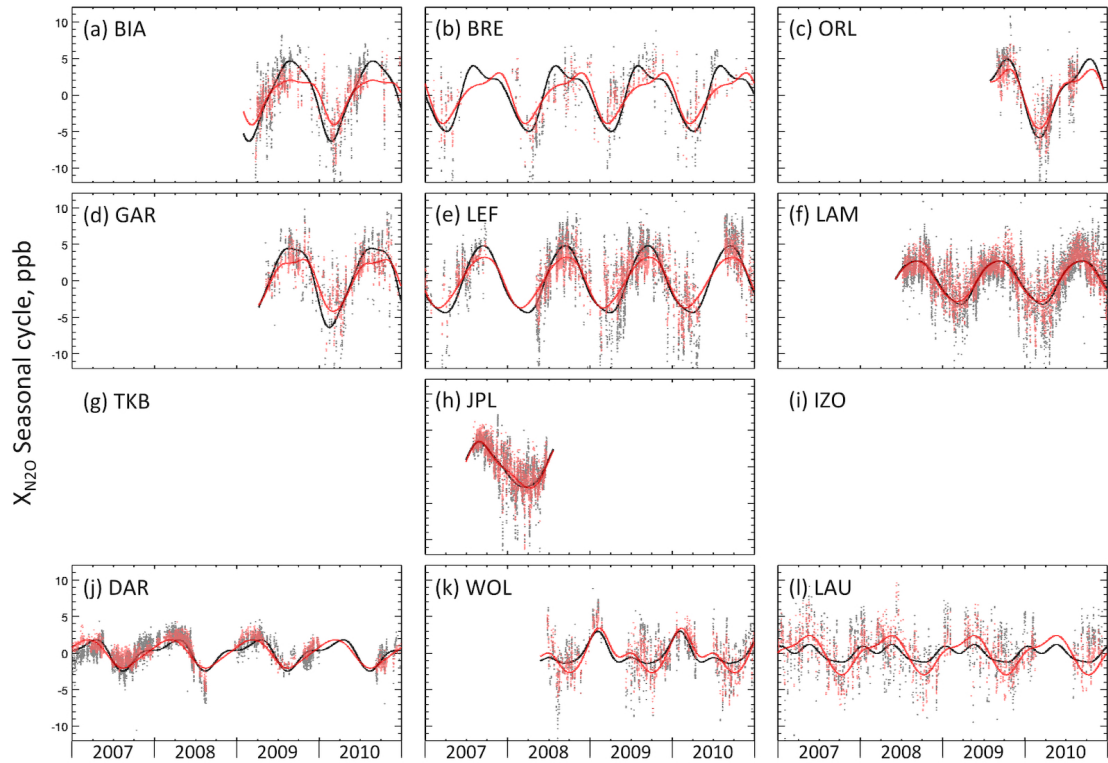


**Figure S7:** Same as Fig. S5, but the seasonal cycles of  $X_{N2O}$  are shown. No  $X_{N2O}$  data are retrieved for KAR, TKB and IZO.

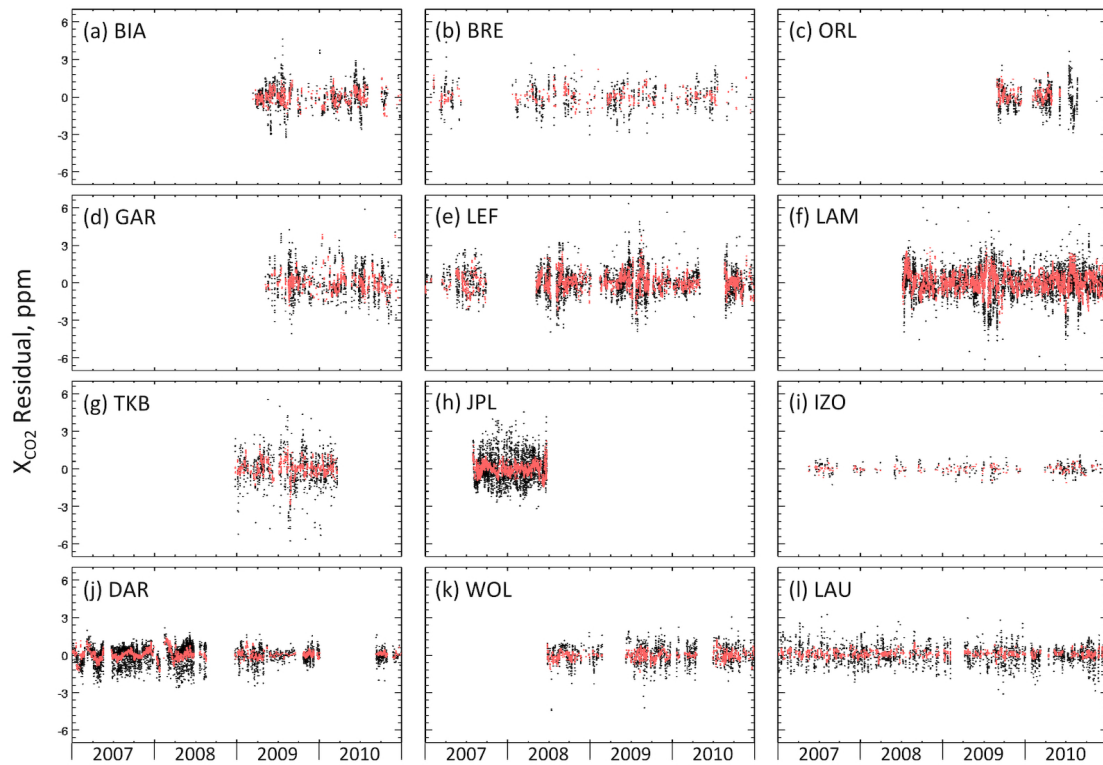


**Figure S8:** Time series of  $X_{CO_2}$  residuals (original time series – fitted curve)

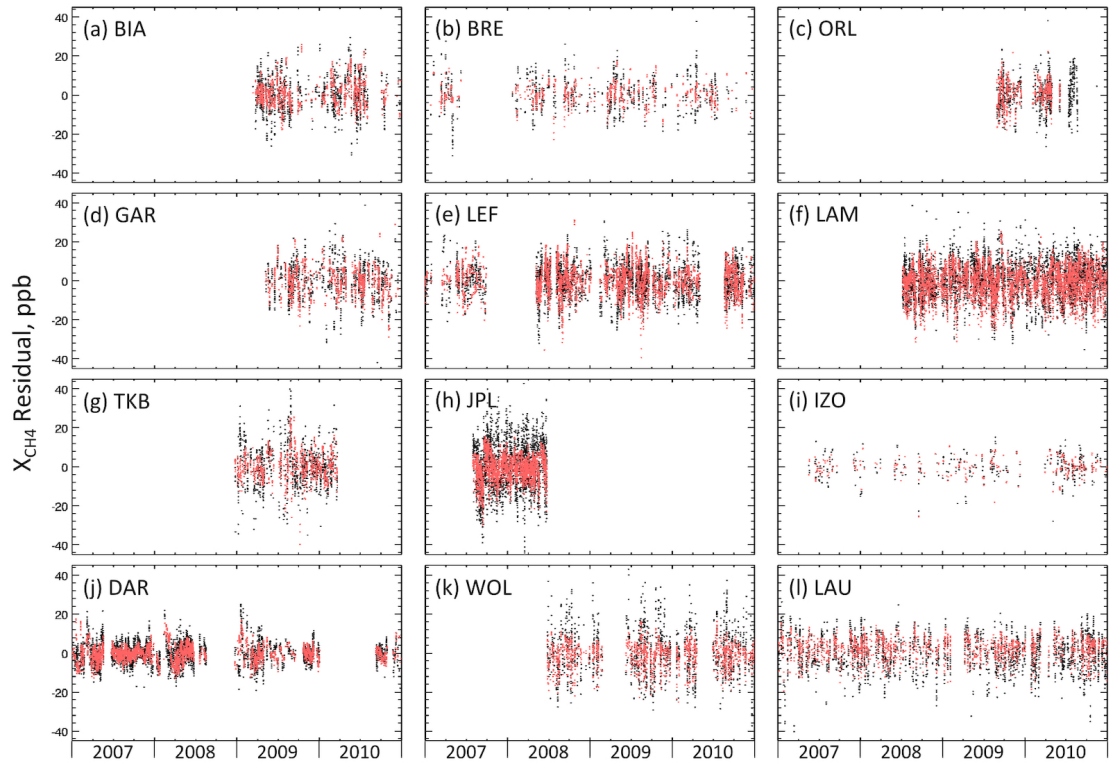


**Figure S9:** Time series of  $X_{CH_4}$  residuals.

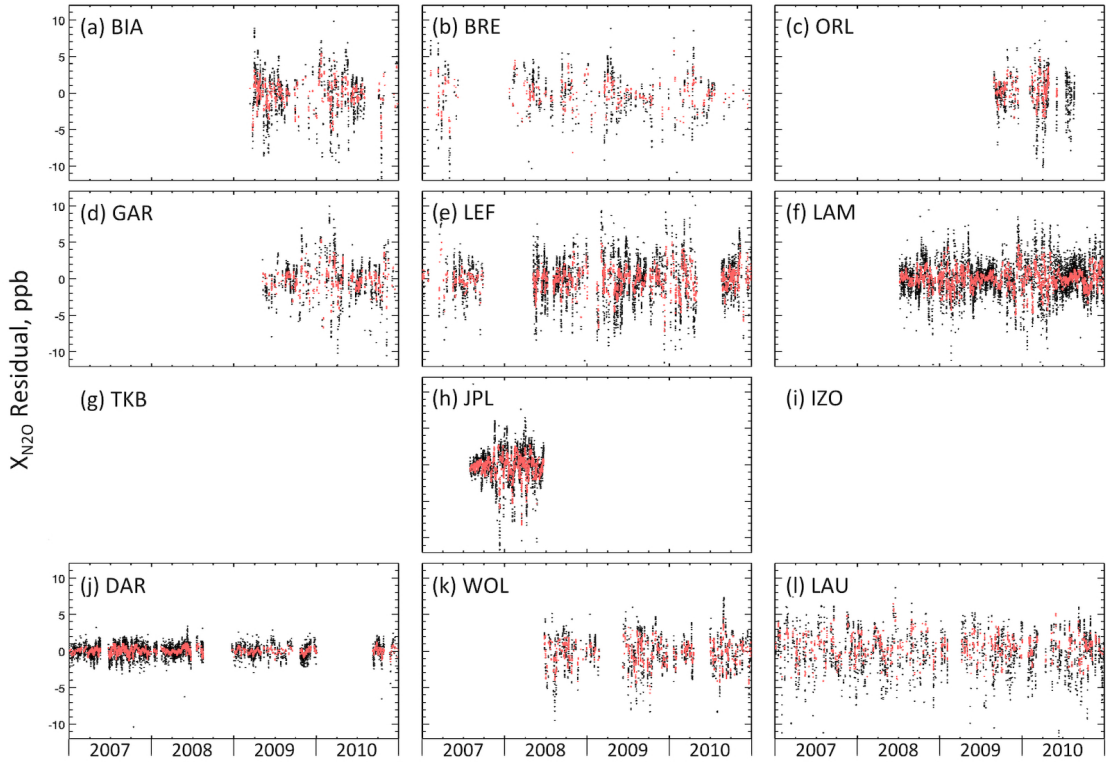


**Figure S10:** Time series of  $X_{N2O}$  residuals.

We have also calculated the partial columns, normalized by the surface pressure, as opposed to normalization by the partial pressures of the troposphere and stratosphere (Eqn. 2 and 3). The tropopause height over the FTS sites are chosen to vary with month as well as kept constant at the annual mean tropopause height.

$$X_{y,tropo} = PC_{y,tropo}/P_s \quad (\text{Eqn. S2})$$

$$X_{y,strato} = PC_{y,strato}/P_s \quad (\text{Eqn. S3})$$

In this calculation the tropospheric and stratospheric partial columns add to the total column.

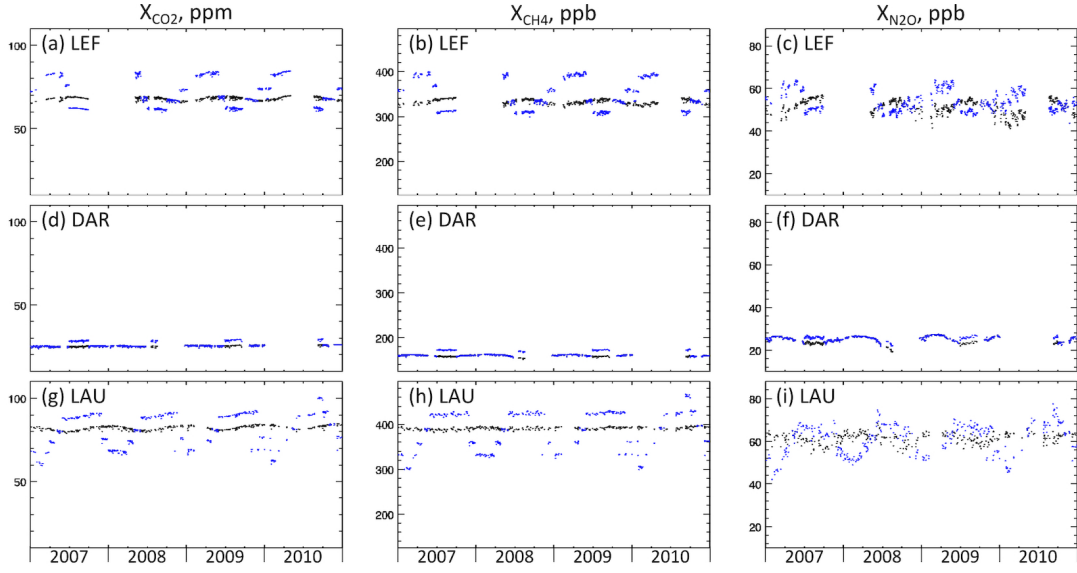


**Figure S11:** Time series of  $X_{CO_2,strat}$ ,  $X_{CH_4,strat}$  and  $X_{N_2O,strat}$  at three selected sites (black for annual mean tropopause, blue for tropopause varying monthly). Similar to Fig. 6, but using a different methodology for calculating stratospheric partial column (see above).

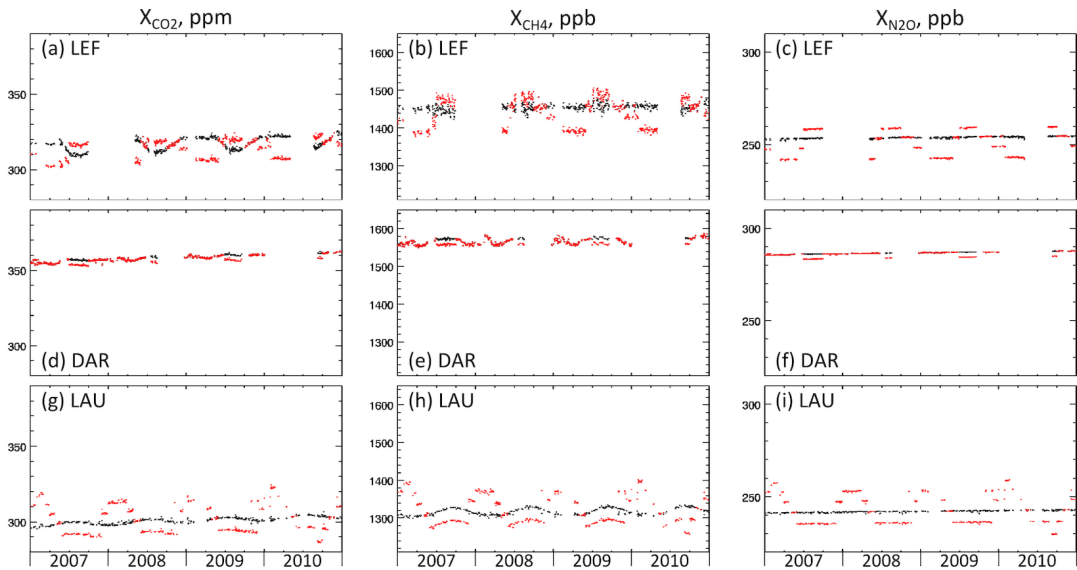


**Figure S12:** Time series of  $X_{CO_2,trop}$ ,  $X_{CH_4,trop}$  and  $X_{N_2O,trop}$  at three selected sites (black for annual mean tropopause, red for tropopause varying monthly).